Stratosphere-troposphere transport in a numerical simulation of midlatitude convection

Article

Accepted Version

JOURNAL OF GEOPHYSICAL RESEARCH, VOL. 112, D06314, doi:10.1029/2006JD007265, 2007

Stratosphere-troposphere transport in a numerical simulation of midlatitude convection

Jeffrey M. Chagnon[1] and Suzanne L. Gray[1]

Received 6 March 2006; revised 26 May 2006; accepted 5 October 2006; published 31 March 2007.

[1] The transport of stratospheric air deep into the troposphere via convection is investigated numerically using the UK Met Office Unified Model. A convective system that formed on 27 June 2004 near southeast England, in the vicinity an upper level potential vorticity anomaly and a lowered tropopause, provides the basis for analysis. Transport is diagnosed using a stratospheric tracer that can either be passed through or withheld from the model's convective parameterization scheme. Three simulations are performed at increasingly finer resolutions, with horizontal grid lengths of 12, 4, and 1 km. In the 12 and 4 km simulations, tracer is transported deeply into the troposphere by the parameterized convection. In the 1 km simulation, for which the convective parameterization is disengaged, deep transport is still accomplished but with a much smaller magnitude. However, the 1 km simulation resolves stirring along the tropopause that does not exist in the coarser simulations. In all three simulations, the concentration of the deeply transported tracer is small, three orders of magnitude less than that of the shallow transport near the tropopause, most likely because of the efficient dilution of parcels in the lower troposphere.

Citation: Chagnon, J. M., and S. L. Gray (2007), Stratosphere-troposphere transport in a numerical simulation of midlatitude convection, *J. Geophys. Res.*, *112*, D06314, doi:10.1029/2006JD007265.

1. Introduction

[2] The chemistry of the lower stratosphere and upper troposphere is sensitive to episodes of cross-tropopause mass transport. This sensitivity arises because of the large contrast in air characteristics on either side of the tropopause. For example, the concentration of ozone has been observed to jump across the tropopause from trace levels in the troposphere, whereas water vapor is abundant in the troposphere and scarce in the stratosphere.

[3] *Holton et al.* [1995] review the various dynamical processes that lead to stratosphere-troposphere exchange (STE) on the global scale, including the role of the Brewer-Dobson circulation in inducing upward mass flux in the tropics and downward mass flux in the extratropics. Observational evidence [e.g., *Stohl et al.*, 2003a] suggests a wide range of temporal and spatial scales on which STE can occur, and also indicates a wide range of associated dynamical processes that may accomplish or encourage local transport events. In the extratropics, exchange events occur frequently within midlatitude cyclones, upper level jets, cutoff lows, and tropopause folds (for a review, see *Stohl et al.* [2003b]). Most of these exchange events are relatively shallow. These larger-scale features represent the context for STE, but smaller-scale (faster) phenomena embedded therein may account for much of the total exchange. The smaller-scale processes may be associated with mixing (e.g., turbulence generated by gravity waves [*Moustaoui et al.*, 2004] or convective updrafts/downdrafts [*Mullendore et al.*, 2005; *Reid and Vaughan*, 2004]) or with local potential vorticity (PV) sources and sinks (e.g., the diabatic generation of a negative PV anomaly near the tropopause and concomitant elevation of the PV-defined tropopause [e.g., *Wirth*, 1995; *Lamarque and Hess*, 1994]).

[4] *Gray* [2003] analyzed the mechanisms by which STE is achieved in a sophisticated numerical weather prediction model. Using an online tracer (i.e., a tracer whose evolution is predicted within the modeling system, rather than via an offline postsimulation analysis of model output), she found that up to half of the total STE in a two day simulation of north Atlantic weather systems (including three baroclinic frontal systems) was accomplished by subgrid-scale parameterized processes. The model's convective scheme accounted for a large proportion of this parameterized transport.

[5] The purpose of this paper is to further investigate the role that convection may play in transporting stratospheric tracer into the troposphere. In particular, we examine the hypothesis that convection may facilitate deep transport of stratospheric air to near-surface elevations, and we analyze the sensitivity of transport estimates by a numerical model to the manner by which convection is represented. Convection may lead to transport for the following reasons. Extratropical convection often takes place in the vicinity of an upper level PV anomaly and an associated tropopause fold. These folds can be quite deep, frequently extending to the 700 hPa pressure level. The deep and turbulent circulations within the convective system, taking place near such a

[1]Department of Meteorology, University of Reading, Reading, UK.

0148-0227/07/2006JD007265$09.00

Table 1. Summary of Model Configurations for the Three Simulations

	Simulation		
	A	B	C
Δx, km	12	4	1
Start time (on 27 Jun 2005), UT	0100	1600	1600
Lateral boundary condition source	global model	simulation A	simulation B
Horizontal grid points (EW $\times$ NS)	146 $\times$ 182	188 $\times$ 126	400 $\times$ 380
Vertical levels	38	38	76
Δz at z = 8 km, m	820	820	405
Convective parameterization scheme status	on	on	off
Horizontal diffusion (order, value)	none	none	4th, 1.43×10^3 m^4 s^{-1}

lowered tropopause, imply a possibility for deep exchange that warrants investigation. Observational evidence for deep stratosphere-to-troposphere transport (STT) by convection has been presented for the southern tropical Indian Ocean [*Randriambelo et al.*, 1999], where lower tropospheric ozone values were measured as high as 200 ppbv, several times larger than is typical. (*Randriambelo et al.* [1999] were not able to attribute this tropospheric ozone unambiguously to deep transport. Other sources, such as biomass burning, were also possible.) Investigations of deep exchange in the extratropics have examined troposphere-to-stratosphere transport (TST) of boundary layer air within the warm conveyor belt region of extratropical cyclones [*Sprenger and Wernli*, 2003]. *Mullendore et al.* [2005] presented an idealized numerical modeling study in which boundary layer tracers were shown to penetrate the tropopause and find a level of neutral buoyancy in the stratosphere. The present study concerns STT by convection in the vicinity of a lowered tropopause.

[6] This study comprises a numerical investigation of stratospheric tracer transport, the basis for which is a case study of a convective event that took place on 27 June 2004 over southern England and the North Sea. The convection initiated and organized near a lowered tropopause and an associated upper level potential vorticity anomaly. The model employed is the (UK) Met Office Unified Model (UM), version 5.5, which is nonhydrostatic, compressible, and parameterizes convection via the mass-flux scheme of *Gregory and Rowntree* [1990]. Note that the study by *Gray* [2003] used version 4.5 of the UM which is hydrostatic and, unlike version 5.5, used an advection scheme for tracers that was different from that used for other the dynamical variables.

[7] The paper is organized as follows. Section 2 describes the essential qualities of the numerical model viz. simulation of STT. Specifically, an online tracer is incorporated in the model that may be passed through the convective and boundary layer parameterizations. Section 3 introduces the case study by presenting the available observational data during the period of interest. Section 4 presents the results from model simulations with horizontal grid lengths of 12 km (the present operational standard), 4 km, and 1 km. Section 5 discusses these results and suggests avenues for additional study.

2. Model Configuration and Strategy

[8] The (UK) Met Office Unified Model (UM) version 5.5, an operational forecasting model employed by the Met Office, was used to simulate the convective system described in section 3. The UM v.5.5 solves the nonhydrostatic, compressible equations of motion on an Arakawa C-grid and a terrain-following Charney-Phillips vertical grid using a semi-implicit semi-Lagrangian temporal integration scheme (see *Davies et al.* [2005] for a detailed description of the dynamical core). With the exception of the density field, all prognostic variables, including tracers, use cubic Lagrange interpolation. We use the standard suite of physics schemes employed by the operational UM, e.g., boundary layer parameterization [*Lock et al.*, 2000]; radiation scheme [*Edwards and Slingo*, 1996]; and the mass-flux convective parameterization [*Gregory and Rowntree*, 1990]. The trigger for this convective parameterization is dependent on the initial parcel buoyancy. The total mass flux in a hypothetical subgrid-scale cloud ensemble is then calculated assuming a specified timescale for the adjustment of convective available potential energy (CAPE) (usually 30 min). Entrainment and detrainment, as well as diabatically cooled downdrafts, also contribute to the total redistribution of mass (including tracer) within the parameterization.

[9] Three limited area domain integrations are performed on a rotated grid for analysis, each utilizing a progressively finer spatial resolution. Table 1 provides the parameter values chosen for these three integrations and Figure 1 depicts the arrangement of the respective domains. The outermost domain (labeled "A"), corresponding to the run with Δx = 12 km, is the standard operational limited area domain used by the UK Met Office. The initial condition for this outermost domain is provided by a mesoscale analysis at 0100 UT on 27 June 2004, and lateral boundary conditions for this outermost domain are supplied by a global model integration of the UM. Simulation "A" then supplies the lateral boundary conditions for a smaller domain (labeled "B"), for which Δx = 4 km, that proceeds from 1600 UT and captures the convective system during its life cycle (the convective system initiates at approximately 1800 UT). This 4 km configuration is also used operationally by the Met Office. A third simulation (labeled "C") is performed on an even finer grid (Δx = 1 km) whose lateral boundary conditions are supplied by simulation "B." This run is also initialized at 1600 UT, and the domain is stretched sufficiently westward in order to allow for the convection to initiate and organize within the domain. All simulations are run until 0000 UT on 28 June 2004, after which time the convective system rapidly decays. Ancillary data such as orography and vegetation distribution are provided on the 12 km grid; in the 4 km and 1 km runs, these data are interpolated from the 12 km grid.

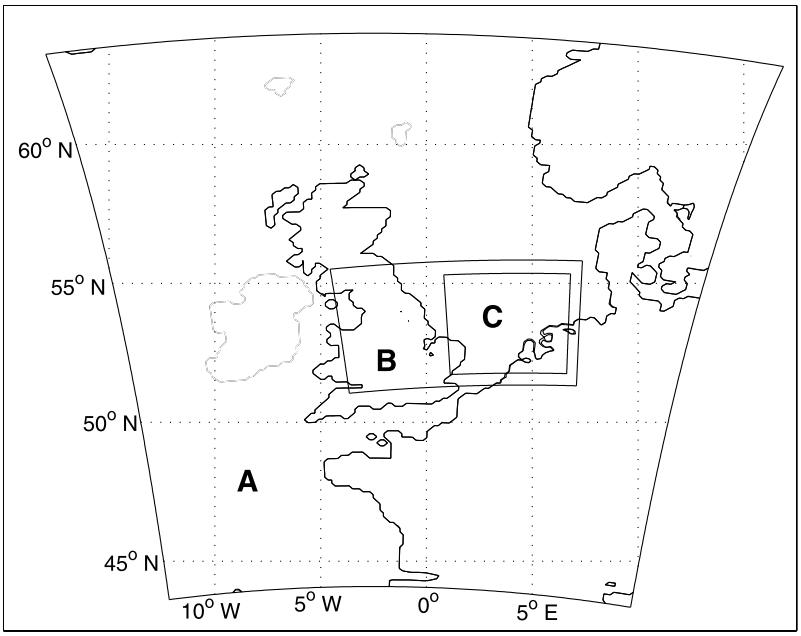

Figure 1. Arrangement of the grids for the simulations A (Δx = 12 km), B (Δx = 4 km), and C (Δx = 1 km).

[10] The diagnosis of cross-tropopause mass transport is accomplished by analyzing an online passive tracer, as opposed to a tracer that is analyzed offline using model output. The advantage of using an online tracer is that it facilitates a prediction of the tracer governed by the same numerical techniques, both physical and dynamical, as the rest of the model variables. Specifically, this implies that (1) the online tracer evolution may be affected by the small-scale, fast processes that may accomplish cross-tropopause transport, such as convection, but must usually be parameterized and (2) the numerical integration schemes that are used to predict the fields that determine the location of the tropopause are also the schemes used to predict the distribution of tracer (see earlier in this section). With respect to the first point above, if we were to use reanalysis winds or grid-scale winds to predict the transport of tracer, then we would not be able to account for small-scale processes. In our model simulations the tracer may be passed through the convective and boundary layer parameterizations and subjected to the mixing implied by these schemes (i.e., a "full physics" tracer). Additionally, we introduce tracers that are withheld from these schemes in order to isolate the contributions from these schemes to the tracer evolution. However, the contribution from the boundary layer scheme to STT was insignificant relative to advection and the convective parameterization scheme and will therefore be dropped from the analysis in the proceeding section.

[11] Although it is clearly advantageous to account for parameterized mixing processes, the clarity of our analysis will retain the uncertainty associated with the parameterizations themselves. By comparing three simulations at progressively higher resolution, some of this uncertainty can be removed. At a horizontal resolution of 12 km the convective parameterization accounts for a large proportion of the rainfall within the convective system. At a resolution of 4 km the convection is still largely parameterized. However, the suitability of the convective parameterization to operate at this awkward resolution is somewhat suspect. In order to avoid accumulation of high values of CAPE at the subgrid-scale, which often leads to unphysical "grid point storms," the convective parameterization has been adapted in the 4 km run following the method of *Roberts* [2003]. Specifically, the CAPE adjustment time is specified as an increasing function of CAPE which consequently ensures that the largest values of mass-flux occur at the smallest spatial scales (i.e., where the CAPE is largest). This parameter adjustment is used in the operational 4 km resolution UM. At a resolution of 1 km the convection scheme is turned off. Although the convection is represented explicitly, the grid-scale convection that develops at this resolution does not produce the full spectrum of turbulent motions [*Bryan et al.*, 2003] that might be vital to STE. This is a liability that we will have to accept if we wish to retain the advantage of simulating a real event in a complicated synoptic-scale environment. Furthermore, at 1 km resolution, the physics schemes have undergone an appreciable amount of testing and parameter tuning by the Met Office (H. Lean, personal communication, 2005) although not to the extent that it is used operationally at this time. Ultimately, these three resolutions afford the ability to examine the direction of convergence of tracer transport.

[12] Diagnosis of STT is accomplished as follows. The tracer is initialized at 0100 UT on 27 June 2004 with a mixing ratio of 1 above the tropopause and zero elsewhere. Any nonzero concentration of tracer existing below the tropopause at a later time is evidence of STT. The tropopause is defined as the 2 PVU surface (1 PVU (potential vorticity unit) = 10^{-6} K m^2 kg^{-1} s^{-1}). As in the interior, the tracer is set in the lateral boundary conditions to a value of 1 above the 2 PVU surface and zero elsewhere. We distinguish between "shallow" exchange and "deep" exchange by integrating tracer in the free troposphere (between the

2 km height and the 1.5 PVU surface near the tropopause) in the former case, and in the lower troposphere (between 50 and 2000 m heights) in the latter case. The 1.5 PVU level was chosen as the upper bound for the free tropospheric tracer integral in order to avoid inclusion of spurious transport across the 2 PVU tropopause where the tracer initially has a step function profile. The 1.5 and 2 PVU surfaces are located by searching downward from the top of the model domain for the first levels at which these values are obtained. In a tropopause fold, the tropopause level may be a multivalued function of height. The search algorithm of *Gray* [2003] is used to find all points connected to the continuous 1.5 and 2 PVU surfaces.

3. Case Description

[13] On the afternoon of 27 June 2004 a region of convection developed near the southeast coast of England and moved eastward into the North Sea toward the coast of the Netherlands. Figure 2 presents the satellite water vapor channel imagery from Meteosat-8 at a time prior to the organization of the convection (1400 UT) and a time after the convective system has formed (2100 UT). At 1400 UT several important features are evident in the water vapor channel imagery (Figure 2a). A warm and dry region, indicated by dark shades over southern England, is the location of a stratospheric intrusion, in this case a tropopause fold. Tropopause folds are a common precursor to convection in midlatitudes because they often imply a potential instability [*Griffiths et al.*, 2000]. Figure 3 presents the skew-T log-p thermodynamic sounding at 1200 UT, near the region where the convective system ultimately organizes (De Bilt, Netherlands), demonstrating a relatively moist and warm layer near the surface capped by a deep layer of dry air in the middle troposphere, a profile characteristic of a potential instability. The profile is also conditionally unstable containing 191 J kg^{-1} of CAPE. The tropopause fold is a region of a positive upper level PV anomaly. The advection of PV at upper levels can force large-scale ascent. These features are of primary relevance to this study because the lowered tropopause implies an increased likelihood of deep STT if convection takes place near the fold.

[14] Several other features of the synoptic weather pattern on 27 June 2004 that are visible in Figure 2a deserve brief mention here, but will not be subsequently treated in much detail. An upper level jet with a northeast-southwest tilted axis is indicated by a cold streak of cirrus clouds that follows the coastline of continental Europe. (The jet is clearly discernible in the model analyzed and simulated upper level winds (not shown).) This jet is associated with the upper level PV anomaly and tropopause fold discussed above. Another obvious feature in the NE corner of Figure 2a is a region of clouds stretched along an axis oriented NW-SE, near which there is moderate precipitation during much of the period of interest (see Figures 4 and 5). (This feature is also evident as a broad deformation axis in the model analyzed and simulated upper level winds (not shown).)

[15] During the hours following 1400 UT, convection forms near the leading edge of the eastward propagating upper level PV anomaly. Sferics data (not shown) demonstrate that the system forms between 1700 and 1800 UT near the southeast coast of England then propagates eastward into the North Sea reaching the coast of the Netherlands before weakening after 0000 UT on 28 June 2004. By 2100 UT on 27 June 2004 the convection has organized into a mature convective system, as indicated in Figure 2b, positioned off the coast of the Netherlands in the North Sea. (Although the convective system does not strictly meet all of *Maddox's* [1980] criteria for a mesoscale convective complex (MCC), it does possess an organized structure characterized by a large region ($>10^6$ km^2) of continuous cold cloud top (<-32 C) for nearly six hours. Mesoscale convective systems occur at a frequency of approximately two per year over the UK and are most likely to form within a so-called "Spanish plume" [*Gray and Marshall*, 1998], although this was not present on 27 June 2004.) The lowered tropopause appears to be located on the southern edge of the convective system. This relationship between the location of the tropopause fold and the convective system, one not uncommon in midlatitude summer, makes this an interesting test case for analyzing STT. In the following sections such an analysis is performed numerically and a more complete depiction of the dynamical context in which this convection formed will be presented.

[16] Figure 4 presents radar-derived precipitation rates (from the Met Office Nimrod data set) at similar times (1500 and 2115 UT) to those shown in Figure 2. These data, which will provide some validation of the numerical simulations in the following sections, corroborate much of what has been discussed above. At 1500 UT (Figure 4a) showers were scattered across the western half of Great Britain, with one stronger cell positioned over South Wales, but no evident large-scale organization. At 2115 UT (Figure 4b) a convective system is positioned over the North Sea near the coast of the Netherlands in the same location as indicated by the satellite water vapor channel imagery (compare to Figure 2b). This convective system is the focus of the analysis presented in the remainder of this paper.

4. Results

[17] This section presents the simulations of the convective system on 27 June 2004, demonstrating the transport of stratospheric tracer in relation to the convective system. The results for the simulations with progressively finer spatial resolution (Δx = 12, 4, and 1 km) are presented in sequence, beginning with the 12 km simulation. The 12 km simulation will be used to identify the larger-scale (i.e., meso-β scale and larger) horizontal (i.e., latitude-longitudinal) dependence of STT on the upper level forcing and the convective system. Because the 12 km and 4 km simulations are qualitatively very similar at the large scale, the vertical dependence of STT and its mechanisms will be explored using the 4 km simulation which provides better resolution and a cleaner analysis at smaller scales. The 1 km simulation will be used to demonstrate the scale dependence of the simulated STE and its related mechanisms when the convective parameterization is inactive. The results at these varying resolutions are discussed and compared in section 5.

4.1. The 12 km Simulation

[18] The general characteristics (e.g., timing, location, spatial extent, and duration) of the simulated convection

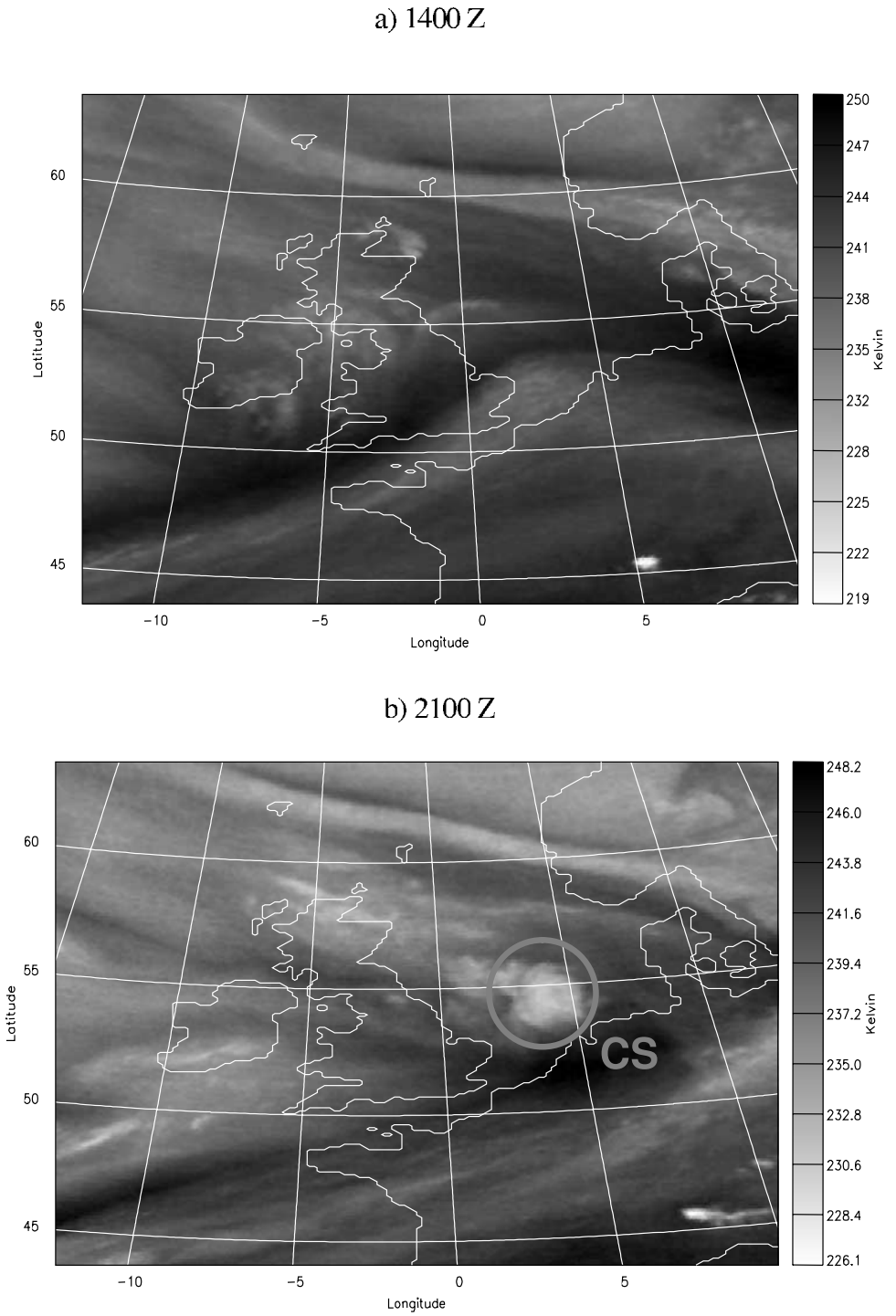

Figure 2. Water vapor channel satellite imagery at (a)1700 UT and (b) 2300 UT on 27 June 2004. The location of the convective system (CS) is annotated in Figure 2b.

compare reasonably well with those that we can infer from the available satellite imagery (Figure 2), sferics data (not shown), and radar data (Figure 4). Figure 5 presents the evolution of simulated rainfall rate from 1500 UT on 27 June 2004 to 0000 UT on 28 June 2004, partitioned between an explicit contribution and that from the convective parameterization. As expected, the parameterized convection contains more structure near the grid scale, whereas the explicit component is relatively smooth. The convective system originates from a region of scattered convection in southeast England between 1500 UT and 1800 UT (see Figures 5e and 5f). During this early stage, there is no explicit component contributing to the rainfall in this region. The scattered nature of the simulated rainfall rate at this early stage (Figures 5a and 5d) resembles that of the radar derived rainfall rate (Figure 4a). After 1800 UT, the region of convective rainfall intensifies and organizes over the North Sea. The organized convective system is partly

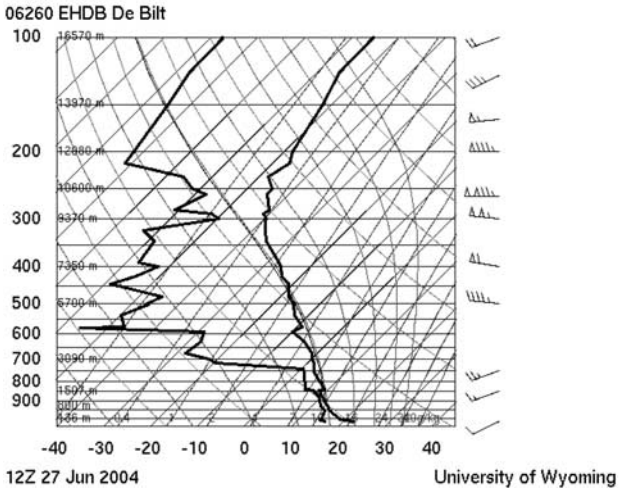

Figure 3. Skew-T log-p thermodynamic profiles at De Bilt at 1200 UT on 27 June 2004 courtesy of the University of Wyoming.

resolved in the simulation, as indicated by the explicit component of rainfall rate after 1800 UT. The total rainfall is approximately partitioned equally between the two components. At 2100 UT, during its mature stage, the general position and size of the simulated convective system compare well to that indicated by the radar data (compare Figures 5c and 5g to Figure 4b). The simulated maximum precipitation rate in this 12 km run (6.1 mm/hr) is less than the 16–32 mm/hr observed by the radar, whereas the 4 km and 1 km runs produce maxima of 34 mm/hr and 90 mm/hr respectively (see below). The radar derived precipitation rate, which is provided on a grid with cells of 4 km by 4 km cross-sectional area, are most appropriately compared to the 4 km run and are expected to yield higher (lower) maximum values when compared to data on a coarser (finer) grid. Although the larger-scale characteristics of the convective system were accurately simulated in all three runs of increasingly finer resolution, the finer details such as maximum precipitation rate were very sensitive to model configuration. Such sensitivity, which may impact the transport of stratospheric tracer by small-scale processes, is a primary motivation for performing the simulation at varying resolution.

[19] The organization of the convective system is most likely accomplished by upper level dynamical forcing associated with a propagating positive PV anomaly. Figure 6 presents the potential temperature on the tropopause (2 PVU) surface, thus demonstrating the location of this upper level PV anomaly and lowered tropopause. Low potential temperatures on the tropopause are a good indicator of a lowered tropopause. A NW-SE oriented axis of low potential temperatures extends from the Atlantic across Ireland to the SW coast of England at 1500 UT (Figure 6a). This lowered tropopause axis moves eastward during the subsequent nine hours, the leading edge of which propagates across southern England and over the North Sea. A comparison between the position of the convective system (Figure 5) and the leading edge of the upper level PV anomaly (Figure 6) demonstrates the correlation between these features. The upper level PV advection was likely to have been a crucial mechanism in the initiation and maintenance of the convective system.

[20] Figure 7 presents the distributions of free and lower tropospheric tracer. The free tropospheric distribution (Figures 7a–7d) suggests that shallow STT takes place mainly in dynamically active regions of the upper troposphere where significant gradients and advection of PV are present. In the southern third of this domain, where there is little upper level activity, there is also very little STT. In the vicinity of the axis of the lowered tropopause (see Figure 6) there are extended ''ribbons'' of free tropospheric tracer. The largest quantities of free tropospheric tracer are located along the southern and downstream edge of the lowered tropopause axis within the tropopause fold. Figure 8 presents a latitude-height cross section of tracer and PV across the axis indicated in Figure 7c at 2100 UT. The tropopause fold, located between 48 and 52°N, is the region where most of the upper level STT has taken place. Another striking feature in Figures 7 and 8 is the east-west extended region of free tropospheric tracer near the northern edge of the domain (e.g., near 62°N in Figure 8). This feature corresponds to the previously mentioned upper level frontal structure evident in the satellite water vapor channel imagery (Figure 2). Although this feature contributes significantly to the transport in the upper troposphere, it is not analyzed in additional detail because it is not convective and does not generate the deep transport which is the focus of this investigation.

[21] The lower tropospheric tracer (Figures 7e–7h) is nonzero near the regions of parameterized rain (compare to Figures 5e–5h). In the vicinity of the convective system, lower tropospheric tracer first occurs at 1800 UT (although at values below the minimum contour level in Figure 7f), then increases in magnitude and spatial extent as the convective system strengthens and organizes following the path of the convective system across the North Sea. In fact, for this 12 km simulation and the 4 km simulation, only the tracer that is allowed to pass through the convective parameterization is transported into the lower troposphere as will be demonstrated below. As mentioned in the previous section, the boundary layer parameterization scheme's contribution to STT is negligible compared to that of the convective parameterization and will thus not be presented for analysis in this paper.

[22] Figure 9 summarizes the phase relationships between the tropospheric tracer, upper level forcing, and the convective system at 2100 UT. A lowered tropopause and upper level PV anomaly stretch NW-SE across England, indicated by the 304 K isentrope on the 2 PVU surface. A convective system forms on the downstream side of this upper level forcing. Within the convective system (parameterized) convection takes place on the leading edge of the system with explicit rain on the trailing side. Additionally, several new (parameterized) convective cells have formed in the rear of the main system. Tracer is transported from the stratosphere to the upper troposphere along the leading edge of the upper level PV anomaly. Most of this upper level tracer is located downstream and south of the convective system. Some tracer is transported deeply into the lower troposphere by the convection. This lower tropospheric tracer is located upstream of the maximum in parameterized rainfall within

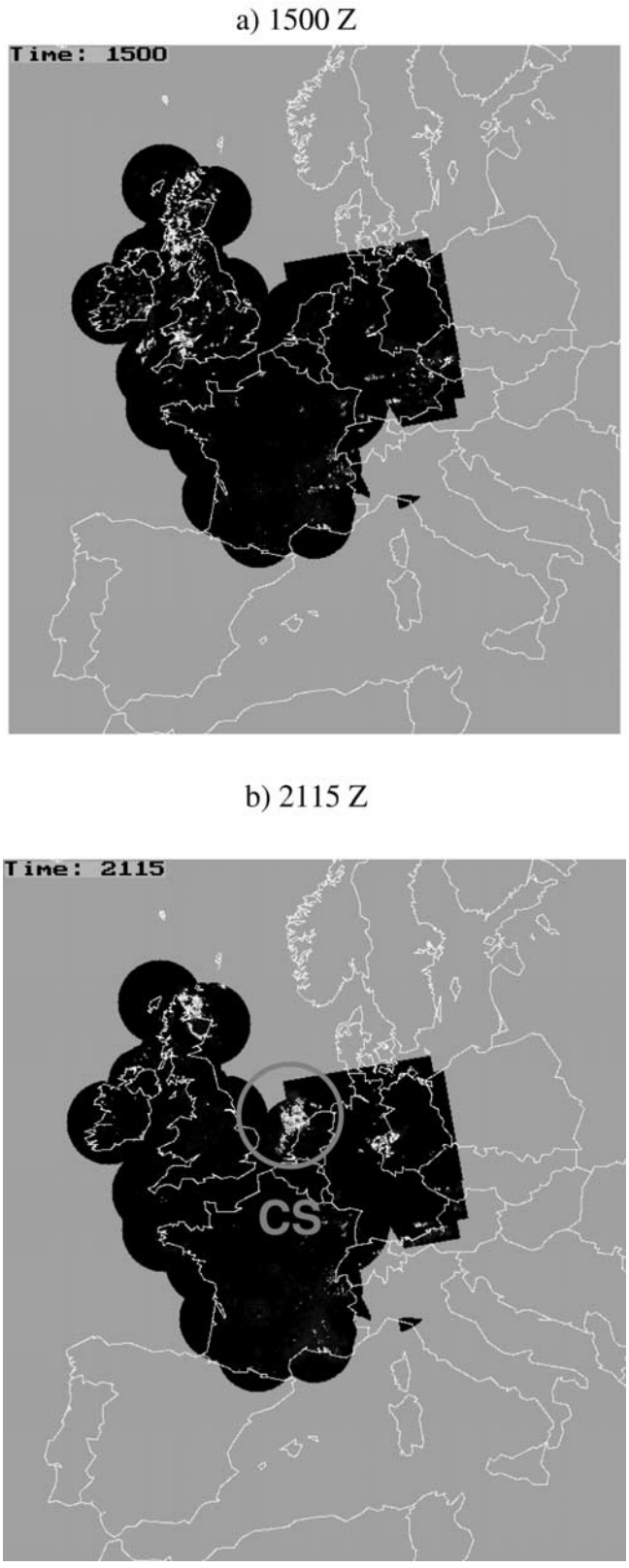

Figure 4. Radar derived rainfall rate at (a)1500 UT and (b) 2115 UT on 27 June 2004 from Met Office Nimrod data set. Peak rainfall rates in the convective system (labeled "CS" in Figure 4b) are between 16 and 32 mm/hr.

the convective system, but is collocated with the developing (parameterized) cells in the rear of the system. Given the horizontal separation between the regions of lower and free tropospheric tracer, it is not likely that the tracer that has been transported to near surface elevation had originated in the fold.

4.2. The 4 km Simulation

[23] The mesoscale characteristics of the convective system in the 4 km simulation are very similar to those in the 12 km simulation presented in section 4.1. This is not very surprising given the importance of the large-scale forcing to this event and that the 4 km simulation is driven by the 12 km simulation through its lateral boundaries. Figure 10 shows the rainfall rate in the 4 km simulation at 2100 UT partitioned between explicit and convective components (as in Figure 5 for the 12 km simulation). The explicit component rainfall rate (Figure 10a) is very similar in position, size, and magnitude to that simulated in the 12 km run (compare to Figure 5c). The convective rainfall (Figure 10b), in spite of having more small-scale structure than in the 12 km simulation (compare to Figure 5g), is similar in position and size to the 12 km simulation. The peak rainfall rate of 34 mm/hr is larger than in 12 km run and compares well to the radar derived estimate (Figure 4c). The general similarities between the 12 and 4 km runs are not very surprising given the extent to which this system was explicitly resolved. Furthermore, the convective parameterization shares a similar burden at these two resolutions in representing the precipitation within the convective system. However, similar the larger-scale characteristics may be, the mass flux, and hence the tracer transport, computed within the convective parameterization need not necessarily be similar at these resolutions.

[24] Figure 11 presents the lower tropospheric tracer in the 4 km simulation. Here, as in Figure 10, we present the distribution of tracer only at 2100 UT because the timing and horizontal transport of tracer in the 4 km simulation is similar to that in the 12 km simulation. The convective system transports some tracer to the lower troposphere over the North Sea in approximately the same quantity as in the 12 km run. A comparison between the position of the convective system (Figure 10) and the location of lower tropospheric tracer (Figure 11a) indicates that the tracer is deposited behind (upstream from) the main region of rain in the convective system, as in the 12 km run. Figure 11b presents a longitude-height cross section of tracer along the dashed axis marked in Figure 11a. The broad upper level region of tracer is evident on the downstream (eastern) side of the main region of deep transport; a deep region of tracer extends to the ground on the upstream (western) side of the convective system.

[25] To examine the role of convection in accomplishing the deep transport of tracer, Figure 12 presents longitude-height cross sections of tracer at 2100 UT along the dashed axis marked in Figure 11a. Note that the region where deep transport takes place is not collocated with the region of maximum free tropospheric tracer (see Figure 7c). The free tropospheric transport (shallow STT) is not a necessary precursor to deep transport. The intent here is to demonstrate the role of specific portions of the convective parameterization in transporting tracer. The parameterization is

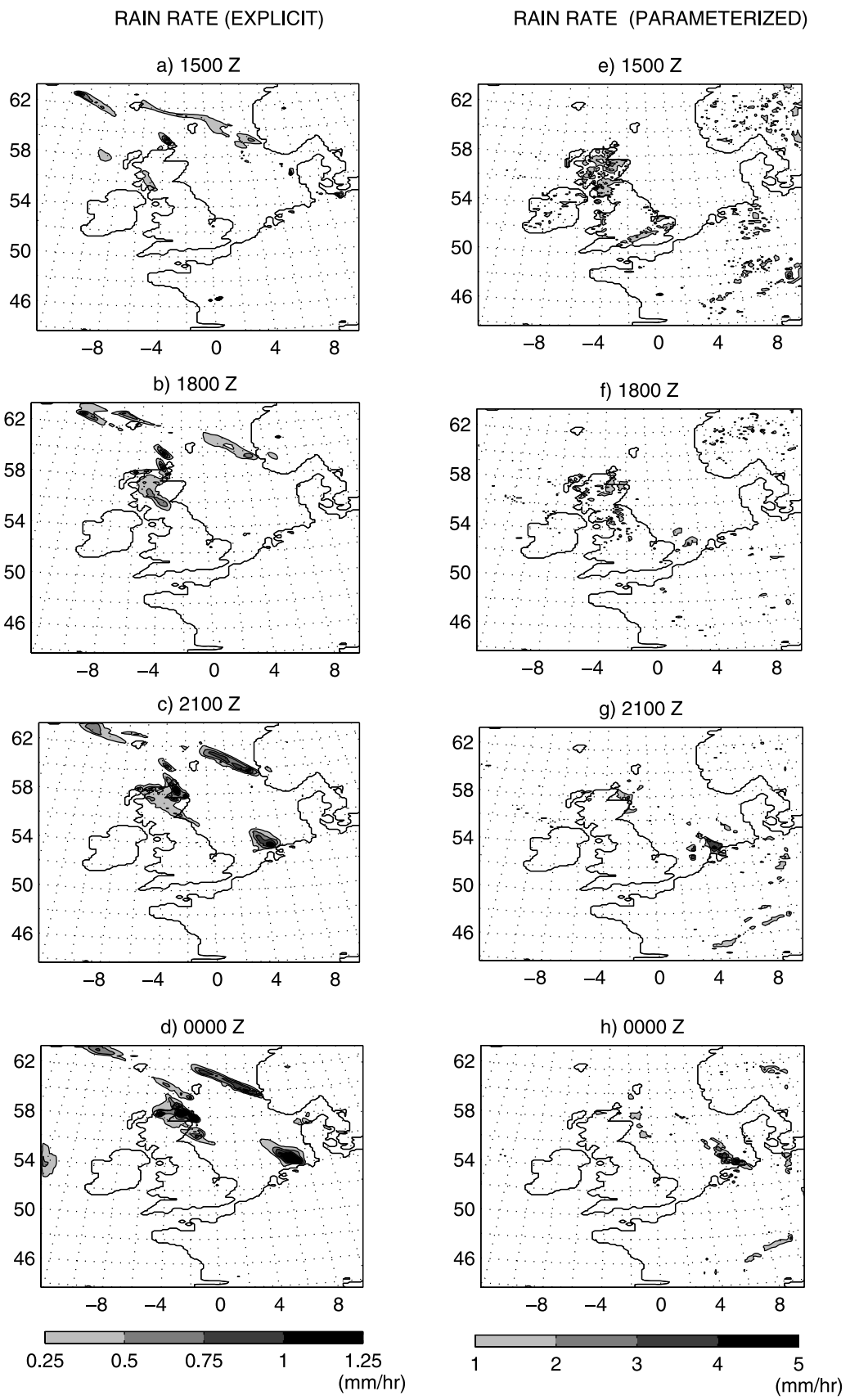

Figure 5. (a–d) Explicit and (e–h) parameterized rainfall rates in the 12 km simulation at 1500 UT (Figures 5a and 5d), 1800 UT (Figures 5b and 5f), and 2100 UT on 27 June 2004 (Figures 5c and 5g) and 0000 UT on 28 June 2004 (Figures 5d and 5h).

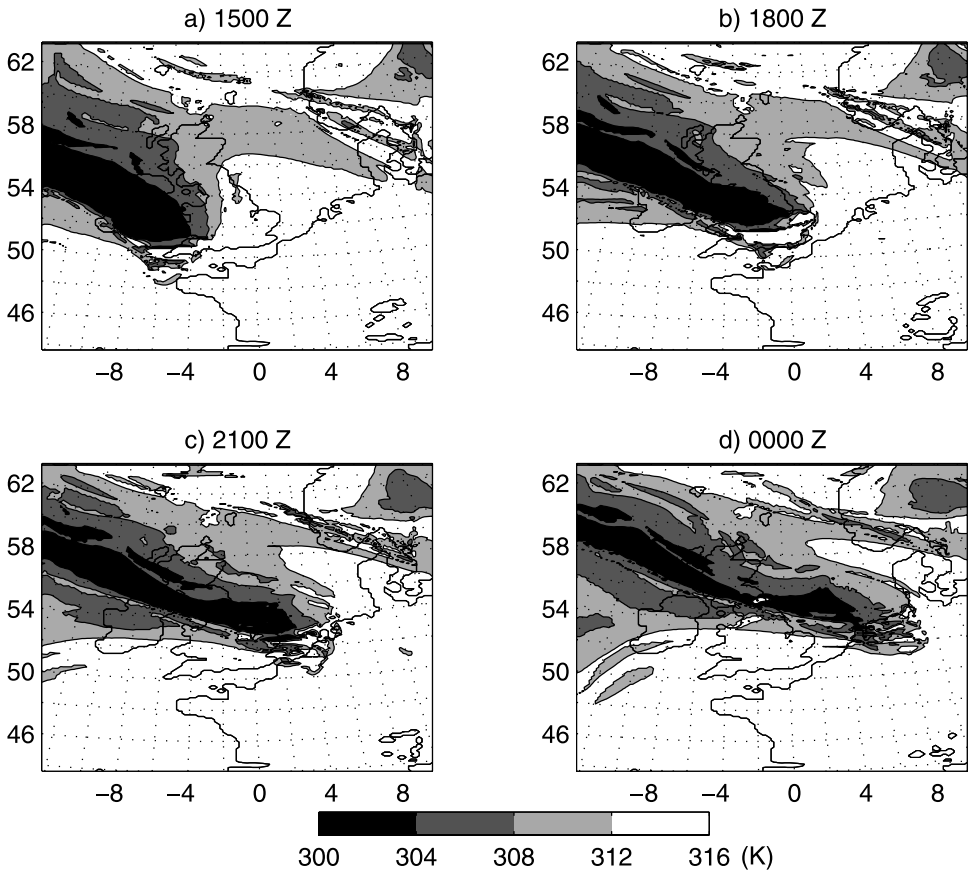

Figure 6. Potential temperature on the tropopause (2 PVU surface) in the Δx = 12 km simulation at (a) 1500 UT, (b) 1800 UT, and (c) 2100 UT on 27 June 2004 and (d) 0000 UT on 28 June 2004.

composed of three main parts that represent distinct physical processes: a bulk cloud ensemble mass flux that accounts for the total redistribution of mass by the turbulent cloud ensemble including both upward and downward local fluxes, a moist downdraft routine that accounts for the microphysically driven downdrafts, and a large-scale adjustment intended to smooth the dynamical response of the grid scale to the perturbations induced by the parameterization. The contribution of the large-scale adjustment to the tracer transport is very small relative to the two other processes and will not be discussed further.

[26] The total convective transport is given by the difference in distributions between the full physics tracer and the tracer that is withheld from the convective parameterization scheme. This difference field can be decomposed into source regions (negative differences, where the scheme reduces tracer concentration, plotted here as absolute values for convenience) and deposit regions (positive differences, where the scheme contributes an increase in tracer). The term source should be interpreted carefully. It may represent either regions from which the tracer has been removed or regions into which clean air has been injected.

[27] Simulations have also been performed in which the tracer has been withheld from the moist downdraft part of the convection scheme. The difference in distributions between the full physics tracer and tracer withheld from the moist downdraft part of the convection scheme gives the tracer transported by the moist downdraft scheme. The difference in distributions between the tracer withheld from the moist downdraft part of the convection scheme and the tracer withheld from the entire convective parameterization scheme gives the tracer transported by the cloud ensemble. These transports can also be decomposed into source and deposit regions. However, the transport by these two parts of the convection scheme are not independent; for example, transport by the cloud ensemble, bringing tracer to below the tropopause, appears to be a prerequisite for transport by the moist downdraft scheme.

[28] The role of the parameterized convection in leading to deep transport is shown by comparing the convective source and deposit regions (Figures 12a and 12d) with the total tracer field at this time (Figure 11b). The similarity between the deposit field and the total tracer field shows that virtually all deep transport is accomplished by the convective parameterization. Overall the scheme removes tracer from above the tropopause (marked by the dashed contour in Figure 12) and deposits it throughout the depth of the troposphere below the tropopause. The cloud ensemble part of the scheme primarily brings tracer from above the tropopause to the upper troposphere (Figures 12b and 12e). Moist downdrafts accomplish the deep transport, transporting air from a relatively localized region just below the tropopause to the atmospheric boundary layer (Figures 12c and 12f). A simulation in which tracer was withheld from the cloud ensemble part of the convection scheme but allowed to pass through the moist downdraft part yielded

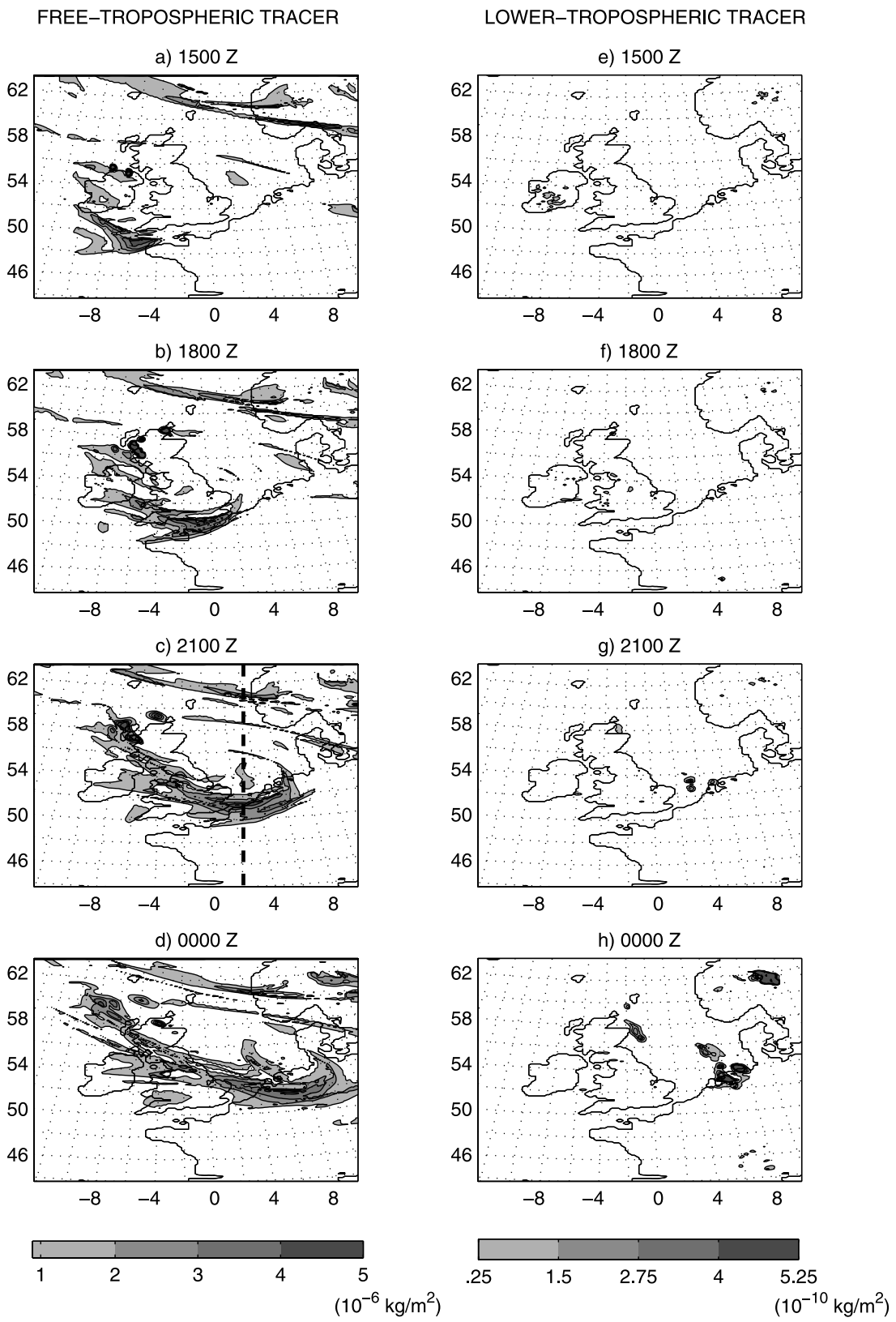

Figure 7. (a–d) Free tropospheric tracer integrated between a height of 2 km and the 1.5 PVU tropopause surface and (e–h) lower tropospheric tracer integrated below an elevation of 2 km in the 12 km simulation at 1500 UT (Figures 7a and 7e), 1800 UT (Figures 7b and 7f), and 2100 UT (Figures 7c and 7g) on 27 June 2004 and 0000 UT on 28 June 2004 (Figures 7d and 7h). The tick dashed axis in Figure 7c marks the cross section used in Figure 8.

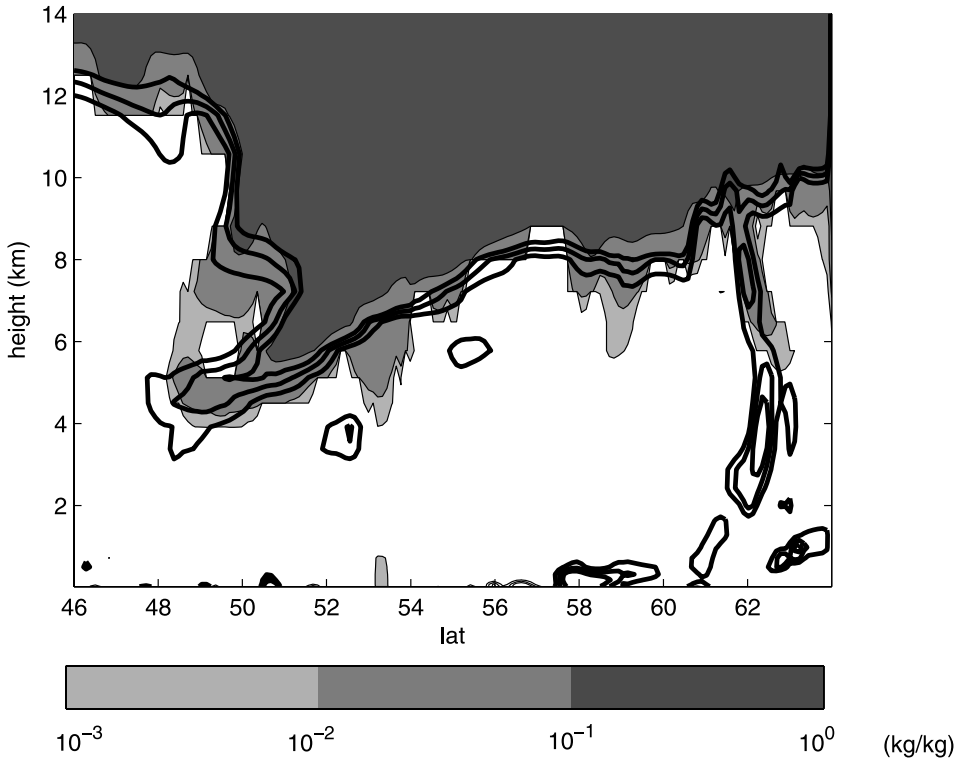

Figure 8. Latitude-height cross section (along the dashed axis depicted in Figure 7c) of tracer (filled contours) and PV (heavy solid contours, values 1, 1.5, and 2 PVU) in the 12 km simulation, valid 2100 UT on 27 June 2004.

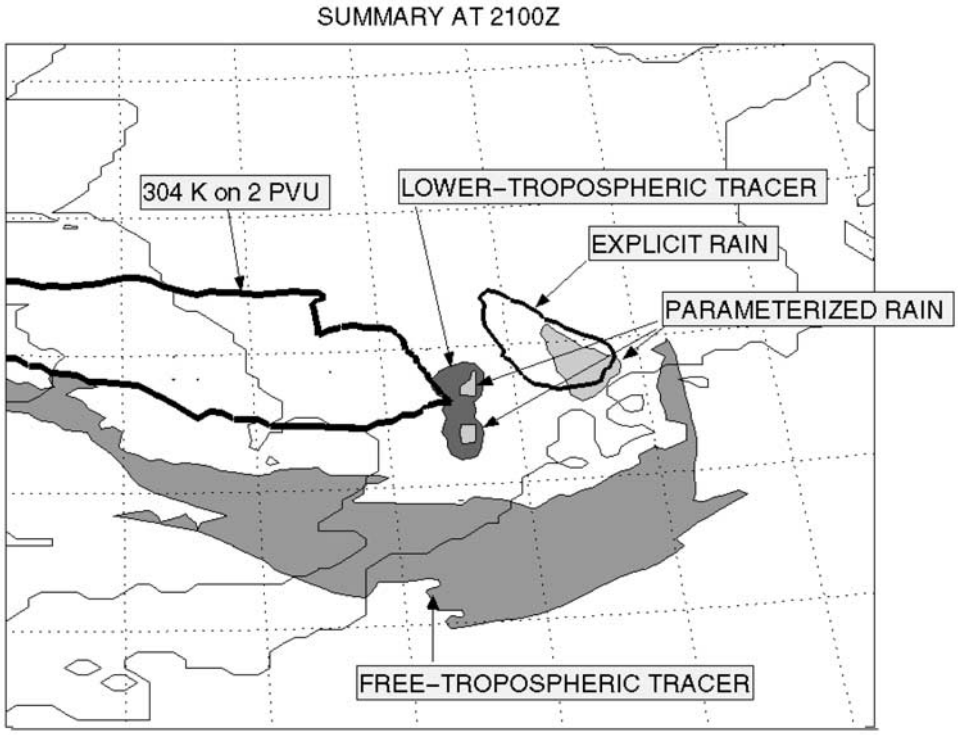

Figure 9. Summary of the phase relationships between various fields in the 12 km simulation at 2100 UT, depicting the position of the lowered tropopause (304 K isentrope on 2 PVU), the explicit rain (.5 mm/hr contour), the convective rain (.5 mm/hr contour), the lower tropospheric tracer (10^{-6} kg/m^2 contour), and the free tropospheric tracer (1.5×10^{-10} kg/m^2 contour).

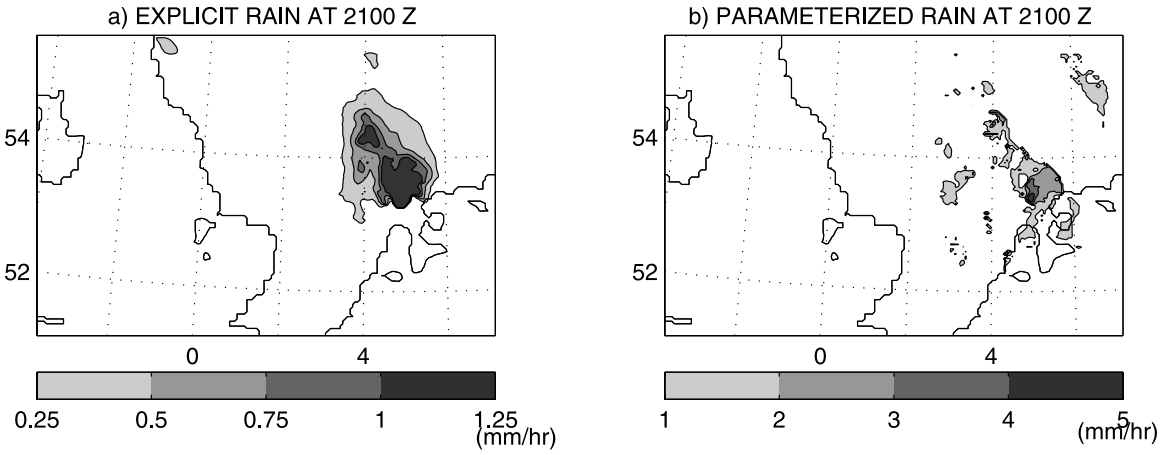

Figure 10. (a) Explicit and (b) parameterized rainfall rate in the 4 km simulation at 2100 UT on 27 June 2004.

no deep transport (not shown). This confirms that shallow transport by the cloud ensemble is a requisite for deep transport by the moist downdrafts.

4.3. The 1 km Simulation

[29] The 1 km simulation is distinguished from the 4 and 12 km simulations in one very important respect: the convective parameterization is disengaged from the modeling system, such that convection is entirely explicit. Any deep STT is accomplished by the resolved dynamics, not through a downdraft routine within a subgrid-scale scheme. The caveat is that 1 km is an inadequate resolution for representing the full turbulence spectrum, thus we cannot have full confidence in the simulated mass flux. This is an acceptable price to pay for having a model capable of simulating convection without a parameterization scheme and which is driven by realistic synoptic forcing.

[30] Figure 13 displays the rainfall rate and lower tropospheric tracer in domain C at 2200 UT. As in the 4 and 12 km simulations, the convection forms at shortly before 1800 UT near the southeast coast of England (not shown) and proceeds to organize and intensify as it moves across the North Sea. The peak rainfall rate at 2100 UT of 90 mm/hr is several times larger than in the 4 and 12 km simulations. (Rainfall rates averaged over a 12 × 12 square of grid boxes in the 1 km simulation are also larger than in the 12 km simulations but compare well to the 4 km run and radar derived estimates.) Additionally, the 1 km simulation produces finer scale structures that are not resolved by the other simulations. In spite of these expected differences, the mesoscale structure of the rainfall in the 1 km simulation is similar to that simulated at the coarser resolutions. For example, the spatial extent and position, the system velocity, the general SE-NW tilt of the main precipitation axis, and the existence of two maxima in precipitation, one in the north and one in the south of the convective system, are features produced in all three runs. As in the previous

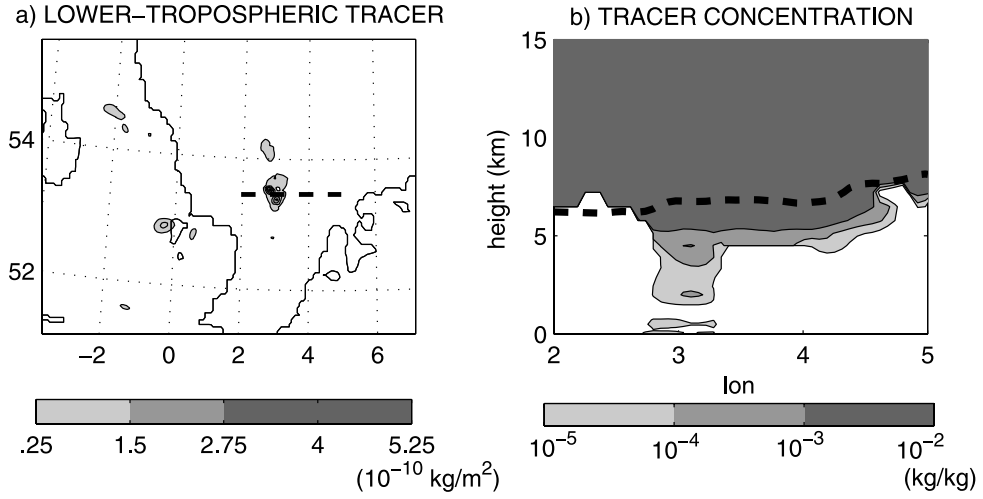

Figure 11. (a) Vertically integrated tracer in the lowest 2 km of the model domain in the 4 km simulation 2100 UT and (b) longitude-height cross section of tracer along the dashed axis shown in Figure 11a.

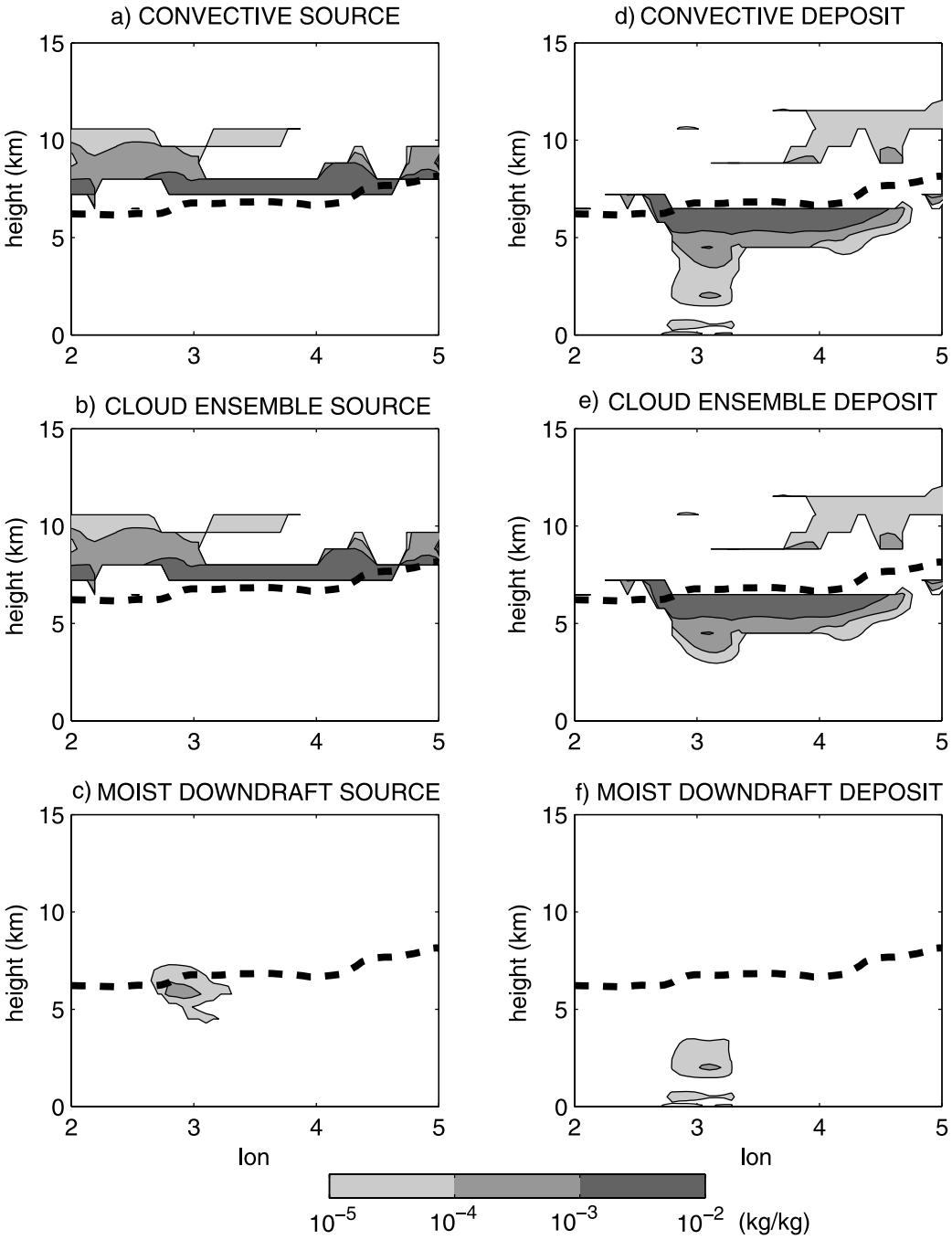

Figure 12. Longitude-height cross section (along dashed axis in Figure 11a) of tracer concentration (filled contours) and 2 PVU (dashed contour) at 2100 UT demonstrating (a–c) source region and (d–e) deposit region owing to total transport within the convective parameterization scheme (Figures 12a and 12d), transport by the mass flux cloud ensemble within the convective parameterization (Figures 12b and 12e), and transport by the moist downdraft routine within the convective parameterization (Figures 12c and 12f).

simulations, the convective system accomplishes some deep transport (Figure 13b). Unlike the previous simulations, this transport must be achieved by the explicitly resolved motions. The magnitude of deeply transported tracer is considerably less (by three orders of magnitude) and occurs several hours later (at 2100 UT) than in the 4 km run. Figures 13c and 13d present a close-up view of the region in which the deep STT takes place (marked by the dashed box in Figure 13b). A comparison of these two frames demonstrates the collocation of the deeply transported tracer with the maximum rainfall rate.

[31] The small-scale dynamics within the convective system are represented quite differently in the 1 km simulation compared to the coarser runs. Figure 14 presents the

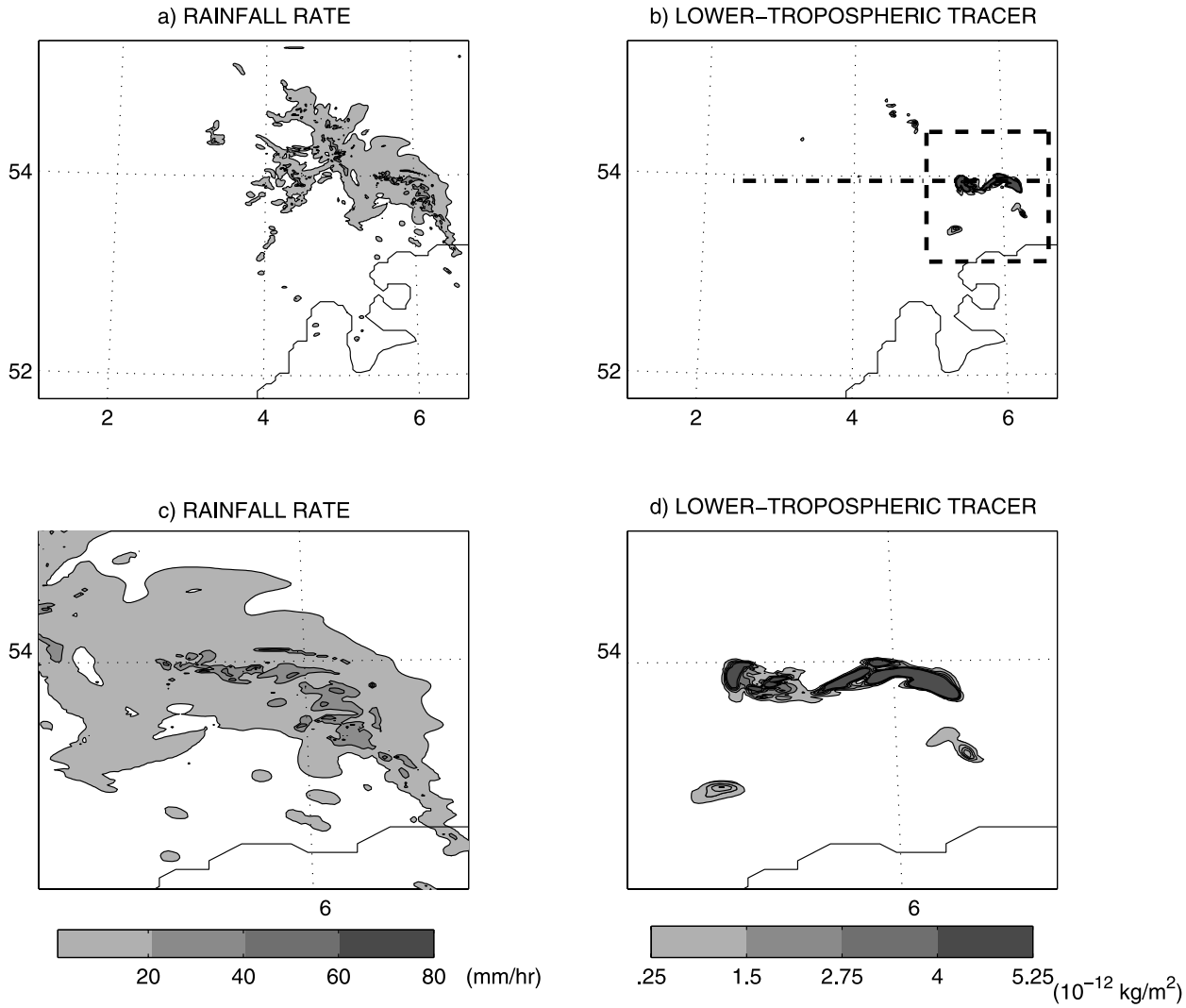

Figure 13. (a) Rainfall rate and (b) lower tropospheric tracer in the 1 km simulation at 2200 UT on 27 June 2004. (c and d) A zoomed in view of Figures 13a and 13b showing the boxed area marked in Figure 13b.

evolution of vertical velocity in the longitude-height cross section intersecting the lower tropospheric tracer (marked by the dotted line in Figure 13b). The poor (1 hour) temporal resolution in Figure 14 makes it somewhat difficult to follow the movement of individual cells, whose timescale is not much longer than 1 hour, but the general movement of the system to the east can nonetheless be observed in this cross section. The tropopause (i.e., the 2 PVU surface) is not shown as it is quite noisy in the vicinity of the convective system because of small-scale sources and sinks of PV. A remarkable feature of the vertical velocity field is that the occurrence of deep convection (i.e., convection reaching to the lowered tropopause at 7 km) is followed by the emergence of wavelike fluctuations along the tropopause. (The ''wavelike'' nature of these fluctuation is clearly apparent in the evolution of vertical velocity on a horizontal surface near the tropopause (not shown).) Figure 15 presents the tracer distribution along the same cross section. The large gradient of tracer at 7 km height is a good indicator of the tropopause position. Between 2000 and 2200 UT (Figures 15b–15d), concomitant to the emergence of vertical velocity fluctuations on the tropopause (Figures 14b–14d), the gradient of tracer at the tropopause becomes noisy and shallow stirring takes place (compare to the smooth distributions at 1900 UT in Figures 14a and 15a). This is a feature that is unresolved by the 4 and 12 km simulations. Furthermore, in the most intense cell, near 5.5°E at 2200 UT (Figure 15d), some of the tracer is transported to near surface levels.

5. Summary and Discussion

[32] The convective event that took place in the afternoon of 27 June 2004 was accompanied by a strong upper level potential vorticity anomaly and a lowered tropopause. The upper level forcing was a likely mechanism for the initiation of the mesoscale convective system that formed near the southeast coast of England and moved into the North Sea toward the coast of the Netherlands. The coexistence of

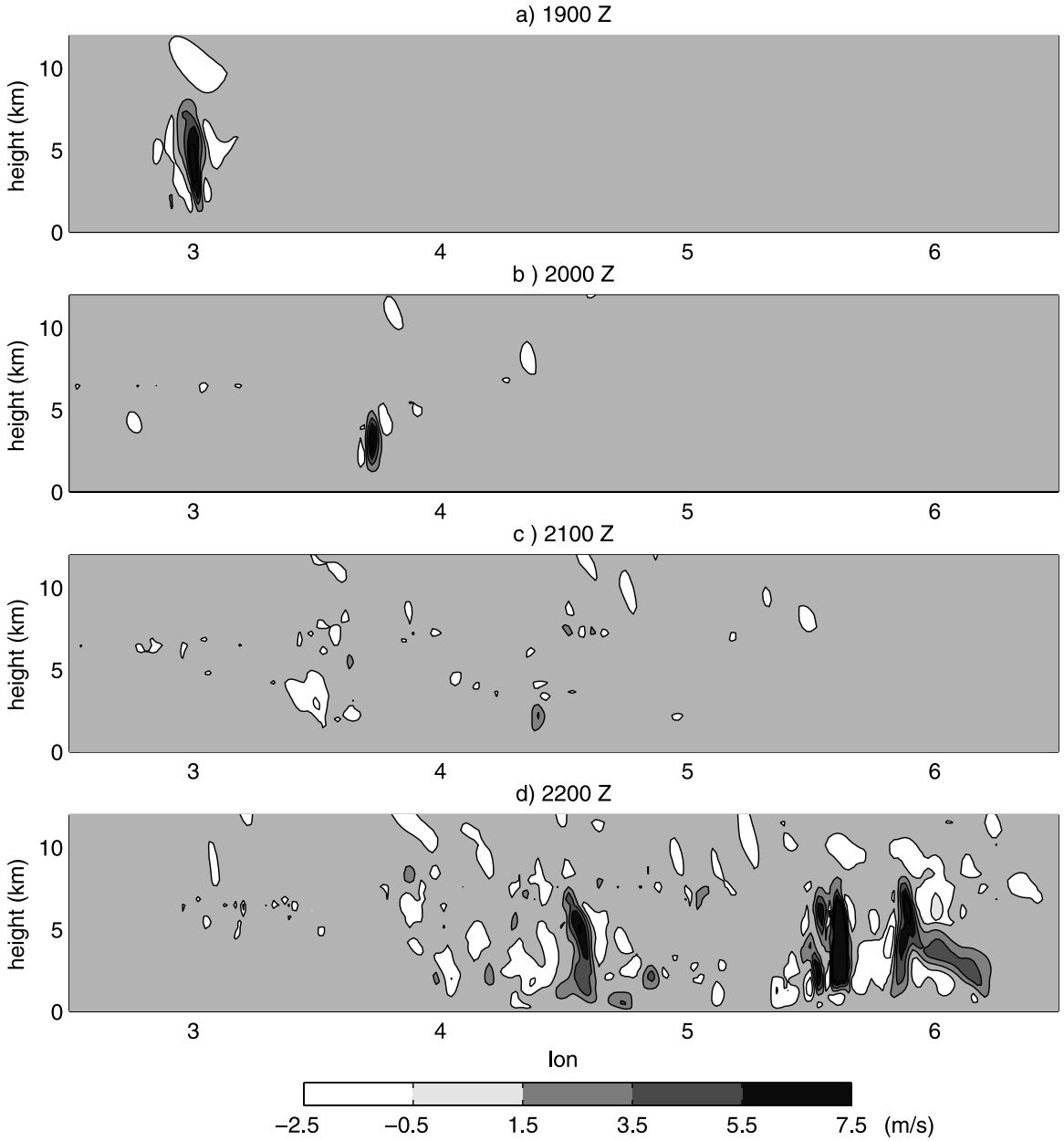

Figure 14. Longitude-height cross section of vertical velocity (along the dash-dotted axis in Figure 13b) in the 1 km simulation at (a) 1900 UT, (b) 2000 UT, (c) 2100 UT, and (d) 2200 UT on 27 June 2004.

these features qualified this case as a good candidate for testing the hypothesis that deep convection near a lowered tropopause can lead to transport of stratospheric air deeply into the troposphere.

[33] Three numerical simulations were carried out in which a tracer was initialized with a mixing ratio of one above the tropopause, and zero elsewhere. The UK Met Office Unified Model was run in its standard mesoscale configuration with a 12 km horizontal grid length. Two additional simulations were performed at higher resolutions in smaller domains that isolated the convective system. These were a 4 km simulation, in which the convective parameterization remained active (although modified to encourage explicit representation of convection only where appropriate), and a 1 km simulation, in which the convective parameterization was disengaged. In the 12 and 4 km simulations, several tracers were utilized. One tracer was only advected by the grid-scale flow via the semi-implicit semi-Lagrangian scheme used for all prognostic variables (excluding density), and the others were passed through the boundary layer and convective parameterization schemes (i.e., ''full physics'' tracer). [Note: the tracer that was passed through only the boundary layer parameterization scheme demonstrated negligible additional contribution to STT and has been dropped from discussion]. The difference between these tracers isolated the contribution of the convective parameterization to the transport of tracer. The tracers were initialized at 0100 UT on 27 June 2004 with a mixing ratio

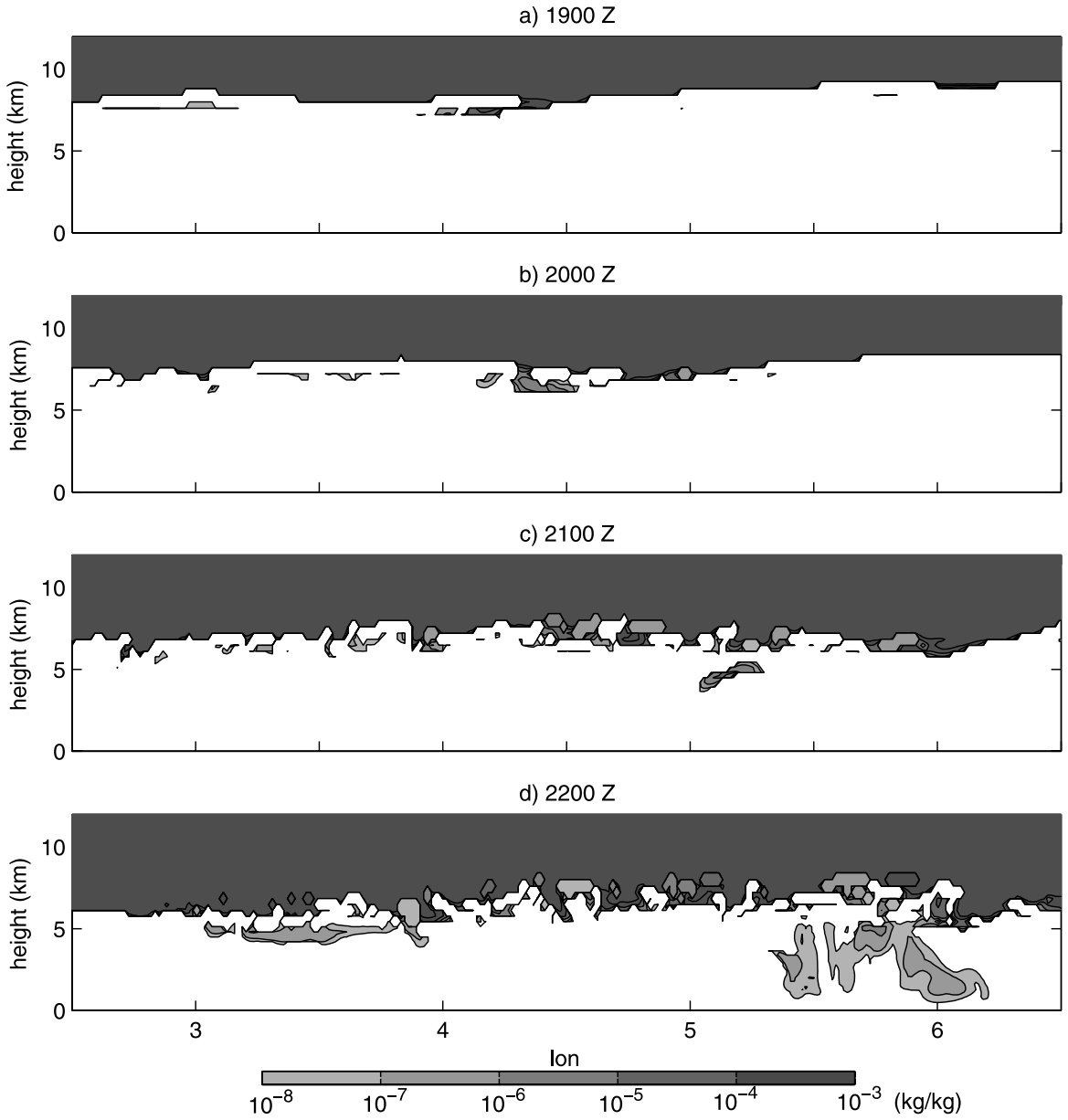

Figure 15. Longitude-height cross section of tracer (along the dash-dotted axis in Figure 13b) in the 1 km simulation at (a) 1900 UT, (b) 2000 UT, (c) 2100 UT, and (d) 2200 UT on 27 June 2004.

of one above the tropopause (here defined as the 2 PVU surface) and zero elsewhere, and similarly in the lateral boundary conditions. A comparison of results in these three simulations reveals the dependence of simulated transport on the model configuration, particularly the spatial resolution.

[34] Deep transport of stratospheric tracer to near-surface levels occurred in all three simulations. In all cases, the tracer transport was accomplished by the deep convective cells. In the 12 km and 4 km simulations this transport was parameterized. The bulk mass flux within the parameterized convective cloud ensemble penetrated the tropopause in most locations where there was convection, removing tracer-rich stratospheric air and depositing it to levels directly beneath the tropopause. In some locations the vertical redistribution extended deeply to near surface levels and was augmented by transport within the parameterized downdrafts. The total transport was largest in the 12 km and 4 km runs, and smallest in the 1 km run. This does not imply that transport at the high-resolution limit will be yet smaller than in the 1 km simulation. *Bryan et al.* [2003] demonstrated that cloud-resolving simulations with grid lengths less than 200 m produce more turbulent convective flows than simulations with 1 km grid length. It is therefore ambiguous as to whether the 1 km simulation is the most reliable and the coarser simulations are less so. Grid lengths lying between 1 and 12 km present an awkward challenge to convective parameterizations which were initially designed to perform at much lower resolution.

[35] In all three simulations, the deep transport of stratospheric tracer through the troposphere occurred without any obvious dependence on preceding large-scale shallow transport into the upper troposphere. The region of primary free tropospheric STT was positioned to the south of the convective system, in the tropopause fold. Shallow transport took place more gradually during the first eighteen hours of the simulation, before the convective system formed. The primary mechanism for this shallow transport was most likely the relatively slow PV generation resulting in negative anomalies above synoptic-scale diabatic sources [*Lamarque and Hess*, 1994]. The lack of colocation between the shallow and deep transport is likely a reflection of their unrelated mechanisms.

[36] The concentration of tracer in the free troposphere was several orders of magnitude larger than that of the tracer that was transported to near surface levels. Mixing efficiently dilutes deeply transported parcels. A parcel exposed to an entrainment rate of 10^{-2} s^{-1} (a value characteristically utilized within the convective parameterization) will dilute by three orders of magnitude within 30 min. The nonmaterial transport that takes place near the tropopause via PV generation does not expose recently transported parcels to an environment as deficient in stratospheric properties as that encountered by a parcel suddenly transported from the stratosphere to the surface; nor are mixing processes as efficient in the upper troposphere. It is therefore unlikely that the deep transport identified in this study will have profound effects on the global calculation of STE. For example, if the stratospheric parcel initially contained an ozone concentration of several hundred ppbv then, after having been transported within our convective system into the lower troposphere, it would have a concentration no greater than a few ppbv above the background, a value indistinguishable to background tropospheric values, and much smaller than the 200 ppbv measured by *Randriambelo et al.* [1999] that was possibly caused by tropical convection.

[37] The 1 km simulation shows small-scale near-tropopause stirring that is unresolved in coarser simulations. The stirring that emerges near the tropopause in the 1 km simulation does so at Richardson number above the critical value of $^1/_4$ (not shown). Furthermore, the stirring is generated only after convection has taken place near the tropopause. Buoyancy waves may provide the link between the convection and emergence of the stirring of tracer. Vertically propagating buoyancy waves cannot be efficiently generated at very coarse resolution, a property owing to their high frequency and relatively large vertical-horizontal aspect ratio. *Lane and Knieval* [2005] demonstrated that a model's ability to generate these waves with sufficient power is sensitively dependent on the model's horizontal resolution; higher-resolution simulations are more likely to contain high-frequency vertically propagating waves. Convection is an efficient generator of high-frequency vertically propagating gravity waves whose origin is the vertical momentum equation [*Lane et al.*, 2001]. It is possible that the stirring of tracer along the tropopause is wave induced, a process that would have been more difficult to simulate in the coarser 4 km and 12 km simulations. Furthermore, it is possible that this wave activity could lead to turbulence and mixing. *Koch et al.* [2005] have recently demonstrated a direct link between gravity waves generated near an upper level jet and the emergence of turbulence. *Reid and Vaughan* [2004] observed enhanced eddy mixing coefficients within turbulence that emerged on the periphery of a tropopause fold that was accompanied by convection over the UK. It is not clear whether the stirring in the present case led to an enhancement of shallow transport, in part because the 2 PVU tropopause surface became very noisy and did not provide an unambiguous boundary separating the troposphere and stratosphere. The potential role of gravity waves in inducing turbulence and mixing along the tropopause is the subject of an ongoing investigation.

[38] **Acknowledgments.** We thank the Met Office for making the UM available. Nigel Roberts and Humphrey Lean of the Joint Centre for Mesoscale Meteorology offered valuable guidance on the high-resolution simulations. Jeffrey M. Chagnon was funded by the Universities Weather Research Network (UWERN) under the NERC Centres for Atmospheric Science (NCAS). Chang-gui Wang (UWERN technical support specialist) supplied diagnostic and visualization tools. Sounding data in Figure 2 were provided courtesy of the Department of Atmospheric Science, University of Wyoming. Met Office Nimrod radar data were supplied by the British Atmospheric Data Centre (BADC).

References

Bryan, G. H., J. C. Wyngaard, and J. M. Fritsch (2003), Resolution requirements for the simulation of deep moist convection, *Mon. Weather Rev.*, *131*, 2394–2416.

Davies, T., M. J. P. Cullen, A. J. Malcolm, M. H. Mawson, A. Staniforth, A. A. White, and N. Wood (2005), A new dynamical core for the Met Office's global and regional modelling of the atmosphere, *Q. J. R. Meteorol. Soc.*, *131*, 1759–1782.

Edwards, J. M., and A. Slingo (1996), Studies with a flexible new radiation code. I: Choosing a configuration for a large-scale model, *Q. J. R. Meteorol. Soc.*, *122*, 689–718.

Koch, S. E., et al. (2005), Turbulence and gravity waves within an upper-level front, *Mon. Weather Rev.*, *62*, 3885–3908.

Gray, M. E. B., and C. Marshall (1998), Mesoscale convective systems over the UK, 1981–97, *Weather*, *53*, 388–396.

Gray, S. L. (2003), A case study of stratosphere to troposphere transport: The role of convective transport and the sensitivity to model resolution, *J. Geophys. Res.*, *108*(D18), 4590, doi:10.1029/2002JD003317.

Gregory, D., and P. R. Rowntree (1990), A mass flux convection scheme with representation of cloud ensemble characteristics and stability-dependent closure, *Mon. Weather Rev.*, *118*, 1483–1506.

Griffiths, M., A. J. Thorpe, and K. A. Browning (2000), Convective destabilisation by a tropopause fold diagnosed using potential vorticity inversion, *Q. J. R. Meteorol. Soc.*, *126*, 125–144.

Holton, J. R., P. H. Haynes, M. E. McIntyre, A. R. Douglass, R. B. Rood, and L. Pfister (1995), Stratosphere-troposphere exchange, *Rev. Geophys*, *33*, 403–439.

Lamarque, J.-F., and P. G. Hess (1994), Cross-tropopause mass exchange and potential vorticity budget in a simulated tropopause folding, *J. Atmos. Sci.*, *51*, 2246–2269.

Lane, T. P., and J. C. Knieval (2005), Some effects of resolution on simulated gravity waves generated by deep, mesoscale convection, *J. Atmos. Sci.*, *62*, 3408–3419.

Lane, T. P., M. J. Reeder, and T. L. Clark (2001), Numerical modelling of gravity wave generation by deep tropical convection, *J. Atmos. Sci.*, *58*, 1249–1274.

Lock, A. P., A. R. Brown, M. R. Bush, G. M. Martin, and R. N. B. Smith (2000), A new boundary layer mixing scheme. Part I: Scheme description and single-column model tests, *Mon. Weather Rev.*, *128*, 3187–3199.

Maddox, R. A. (1980), Meso−convective complexes, *Bull. Am. Meteorol. Soc.*, *61*, 1374–1387.

Moustaoui, M., B. Joseph, and H. Teitelbaum (2004), Mixing layer formation near the tropopause due to gravity wave-critical level interactions in a cloud resolving model, *J. Atmos. Sci.*, *61*, 3112–3124.

Mullendore, G. L., D. R. Durran, and J. R. Holton (2005), Cross-tropopause tracer transport in midlatitude convection, *J. Geophys. Res.*, *110*, D06113, doi:10.1029/2004JD005059.

Randriambelo, T., J. L. Baray, S. Baldy, and P. Bremaud (1999), A case study of extreme tropospheric ozone contamination in the tropics using in-situ, satellite and meteorological data, *Geophys. Res. Lett.*, *26*, 1287–1290.

Reid, H. J., and G. Vaughan (2004), Convective mixing in a tropopause fold, *Q. J. R. Meteorol. Soc.*, *130*, 1195–1212.

Roberts, N. M. (2003), The impact of a change to the use of the convection scheme to high resolution simulations of convective events (State 2 report from the Storm Scale Numerical Modelling Projects), *JCMM Internal Rep.*, *142, Forecasting Res. Tech. Rep.*, *407*, Joint Cent. for Mesoscale Meteorol., Reading, U. K.

Sprenger, M., and H. Wernli (2003), A northern hemispheric climatology of cross-tropopause exchange for the ERA15 time period (1979–1993), *J. Geophys. Res.*, *108*(D12), 8521, doi:10.1029/2002JD002636.

Stohl, A., et al. (2003a), Stratosphere-troposphere exchange: A review, and what we have learned from STOCCATO, *J. Geophys. Res.*, *108*(D12), 8516, doi:10.1029/2002JD002490.

Stohl, A., H. Wernli, P. James, M. Bourqui, C. Forster, M. A. Liniger, P. Seibert, and M. Sprenger (2003b), A new perspective of stratosphere-troposphere exchange, *Bull. Am. Meteorol. Soc.*, *84*, 1565–1573.

Wirth, V. (1995), Diabatic heating in an axisymmetric cut-off cyclone and related stratosphere-troposphere exchange, *Q. J. R. Meteorol. Soc.*, *121*, 127–147.

J. M. Chagnon and S. L. Gray, Department of Meteorology, University of Reading, Reading RG6 6BB, UK. (j.chagnon@reading.ac.uk)